

Arbitrary free spectral range control of optical frequency combs based on an optical tapped delay line structure cascaded with a phase modulator*

WEI Xinhang (韦新航), MU Hongqian (牟宏谦)**, LI Min (李敏), PEI Li (裴丽), WANG Muguang (王目光), and LIU Yan (刘艳)

Key Laboratory of All Optical Network and Advanced Telecommunication Network, Ministry of Education, Institute of Lightwave Technology, Beijing Jiaotong University, Beijing 100044, China

(Received 16 October 2020; Revised 22 December 2020)

©Tianjin University of Technology 2021

We propose and demonstrate a simple method to accomplish arbitrary free spectral range (FSR) control of optical frequency combs (OFC). The approach is based on the combination of an optical tapped delay line (OTDL) structure and a phase modulator (PM). The OTDL structure is utilized to multiply the FSR of input OFC, and the PM is used to divide the FSR of the consequent OFC. We illustrate that the proposed method allows one to divide or multiply the FSR of original OFC by any anticipated integer or fractional factor. Numerical simulation results match well with our theoretical analysis.

Document code: A **Article ID:** 1673-1905(2021)07-0390-5

DOI <https://doi.org/10.1007/s11801-021-0166-7>

Flexibly controlling the key characteristics of optical frequency combs (OFC), such as free spectral range (FSR) and central frequency, is essential for numerous applications, including microwave photonics^[1], spectroscopy^[2,3], frequency metrology^[4,5], and optical signal processing^[6]. OFC is traditionally generated through passively mode-locked laser, which presents a restricted tunability in the frequency offset and FSR. In order to improve the tunability of OFC, diversified solutions have been developed^[7-11]. Among them, spectral Talbot effect, or spectral self-imaging (SSI) effect, is a promising approach to tune the FSR of OFC^[7]. On the other side, temporal self-imaging (TSI) effect has been widely employed to multiply the repetition-rate of optical pulses by applying parabolic spectral phase-only filtering to input pulse trains (typically accomplished by dispersive medium)^[8]. Similarly, SSI will appear when a train of optical pulse is applied a quadratic temporal phase, e.g. through cross-phase modulation or temporal multilevel phase modulation^[9]. Nevertheless, from the view of OFC control, TSI cannot modify the FSR of original OFC, while SSI can only divide the FSR of OFC by an integer factor. In order to achieve a more flexible control of OFC, the combination of TSI and SSI effect has been suggested^[10,11]. In Ref.[10], a quadratic spectral phase is firstly imposed to the input OFC through group-velocity dispersion (GVD), leading to TSI effect. Subsequently resulting Talbot phases of temporal pulse train are compensated via a phase modulator (PM), and at last a

time-domain parabolic phase is imposed to the phase-compensated pulse train via a second PM, leading to SSI effect. In this way, the FSR of input OFC can be divided or multiplied by an expected fractional or integer factor. However, input OFC with relatively low FSR (e.g., in the megahertz regime) requires a very large value of GVD, which is challenging to achieve using current technique. Recently, H. G. de Chatellus use a Talbot laser, which is equal to a mode-locked laser filtered by dispersive medium^[11], to achieve arbitrary control (multiplication or division by any anticipated integer or fractional number) of the FSR of OFC. Although this scheme avoids the use of GVD, its practical system stability is only guaranteed for half an hour.

The optical tapped delay line (OTDL) structure has been extensively utilized in optical time division multiplexing (OTDM) and microwave photonic filtering^[12-14]. It can also be operated to perform spectral amplitude filtering (SAF) for multiplication of pulse repetition-rate. When a train of optical pulse passes through an OTDL structure, which is configured as a spectral amplitude filter, the FSR of comb lines will be increased to an integer multiple of initial FSR, leading to the integer multiplication of pulse repetition-rate. Comparing SAF with SSI effect, we can see that they have opposite effects on the FSR of OFC, which inspires us that it is probable to achieve arbitrary FSR control through the combination of SAF and SSI effect. In this letter, we present a simple approach to implement arbitrary FSR control of input

* This work has been supported by the Fundamental Research Funds for the Central Universities (No.2019JBM010), and the National Natural Science Foundation of China (Nos.61775015 and 61827817).

** E-mail: hongqianmu@bjtu.edu.cn

OFC. The scheme is based on an OTDL structure cascaded with a PM. The OTDL structure is utilized to perform the SAF of the input OFC, implementing the integer multiplication of original FSR. The multiplied FSR is subsequently divided by an integer number based on the SSI effect that is achieved by a PM. Finally, we can obtain the OFC with FSR equal to any expected fractional or integer multiple of initial FSR. Several simulation examples, including integer FSR multiplication, fractional FSR multiplication and fractional FSR division, have been presented. The simulation results verify our theoretical proposal. In addition, the effects of optical delay line inaccuracy and phase noise on the output OFC have also been discussed briefly.

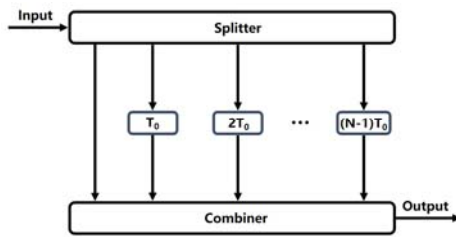


Fig.1 Schematic diagram of optical tapped delay line structure with N taps

The OTDL structure to perform SAF is illustrated in Fig.1. The input optical signal is divided into N paths by a splitter, and each path is delayed by an integer multiple of T_0 , which is set at $1/N$ of the period of input pulse train. All the delayed paths are summed by using a combiner. Compared with the OTDL structures in Refs.[15] and [16], this structure is a simplified version without complex power and phase control of each arm, since the purpose is only the SAF. The frequency response of the OTDL structure can be given by

$$H(\omega) = \frac{1}{N} \sum_{n=0}^{N-1} \exp(-j\omega n T_0). \quad (1)$$

It is obvious that the frequency response is a periodic sinc function with FSR equal to $1/T_0$. As an example, Fig.2(a) and (b) respectively show the power and phase response of OTDL structure for the case $N=4$. It can be seen that except for the maximum transmission points at each integer multiple of the FSR (blue markers), the spectral components at each $1/N$ of FSR (red markers) are suppressed by the spectral amplitude filter. Notice that the overshoot peaks of phase response are artifacts at zero powers. Hence, when a pulse train with the repetition-rate of FSR/N is delivered to an OTDL structure under the condition where the locations of the input comb lines are aligned with the FSR of spectral amplitude filter, the line spacing of output comb will become N multiple of the initial one, and meanwhile input pulse's repetition-rate will also be increased by N times. Here we need to point out that some restrictions have to be imposed to the value of N in practical applications. Firstly, in order to avoid the overlap of adjacent pulses

after SAF, the value of N should not be greater than the ratio of the period to an individual pulse duration of the input train. In addition, since some comb lines are eliminated, the SAF possesses intrinsic loss, which increases as N increases. Therefore, one should take these factors into account when designing practical systems.

Subsequently, SSI effect is introduced by imposing a parabolic phase on output optical pulse train of the OTDL structure, which divides the FSR of filtered OFC by an integer m . The process can be performed through the multilevel phase modulation, i.e., using a PM driven by a multilevel electrical signal. According to the number theory of SSI^[17,18], the phase profile that is imposed to the n th pulse of the input optical pulse train is given by

$$\varphi_n = \frac{s}{m} \pi n^2, \quad (2)$$

where s and m are coprime integers, and m is FSR division factor. Note that the phase values satisfying Eq.(2) can be applied to the whole period of n th pulse or the n th pulse's duration. As a matter of fact, the values satisfying Eq.(2) could be applied no more than 2π through the modulo operation. Moreover, it is easy to see that φ_n is periodic with period m when the product of s and m is even, or with period $2m$ when the product of s and m is odd. In other words, we need to perform a periodic phase modulation that contains m or $2m$ discrete phase levels in each period. Therefore, the period of modulation signal ought to be m or $2m$ multiple of the output pulse period of the OTDL structure. Note that no comb lines shifting occurs when $(s \cdot m)$ is even. However, all comb lines will be shifted by half the FSR of output comb when $(s \cdot m)$ is odd.

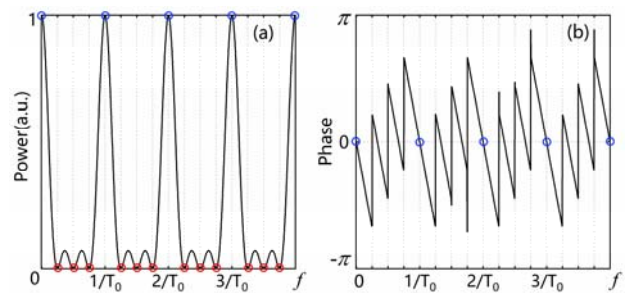


Fig.2 (a) Power response and (b) phase response of the OTDL structure with four taps

Fig.3 illustrates the principle for arbitrary FSR control using an OTDL structure cascaded with a PM. Here our target is to convert an original OFC with FSR f_r to an OFC with FSR $(N/m)f_r$, where N and m are integers we desire. First, a pulse train with the period of $1/f_r$ (Fig.3(a.1)), which corresponds to an OFC with FSR f_r in frequency domain (Fig.3(b.1)), is sent to the OTDL structure to perform the SAF. The result is an OFC with FSR equal to Nf_r (Fig.3(b.2)), leading to the N times multiplication of pulse's repetition-rate, as

shown in Fig.3(a.2). And then a phase sequence satisfying Eq.(2) (SSI condition) is imposed to the multiplied pulse train. This enables the division of the obtained FSR Nf_r by an integer m , leading to an output comb with FSR $(N/m)f_r$, as shown in Fig.3(b.3). By this means, an original OFC with FSR f_r is eventually converted to an OFC with FSR $(N/m)f_r$. Note that the factor N/m can be designed greater or less than 1, so the FSR of initial OFC can be divided or multiplied by any anticipated fraction or integer theoretically.

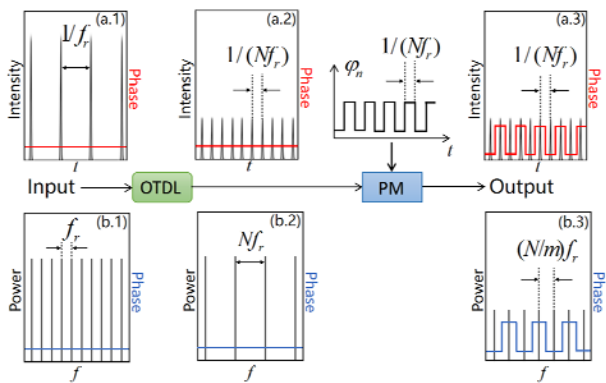


Fig.3 Principle of arbitrary FSR control based on the combination of SAF and SSI in the case for $N=3$, $s=1$ and $m=2$: (a.1)-(a.3) The time-domain pulse trains of input comb, the comb after the OTDL structure and output comb respectively; (b.1)-(b.3) The counterparts in frequency domain of (a.1)-(a.3)

In order to validate the feasibility of proposed arbitrary FSR control method based on the combination of an OTDL structure and a PM, we used the OptiSystem (simulation software) to implement several numerical simulations. As an example, Fig.4 shows the simulation setup to accomplish 2.5-times FSR multiplication. Gaussian pulse train at 1 550 nm with a repetition rate of 10 GHz and pulse-width of 5 ps is used to provide input OFC, which is depicted in black line in both Fig.5 and Fig.6. The consequent output OFC (red lines) are drawn in a linear scale and compared with input combs.

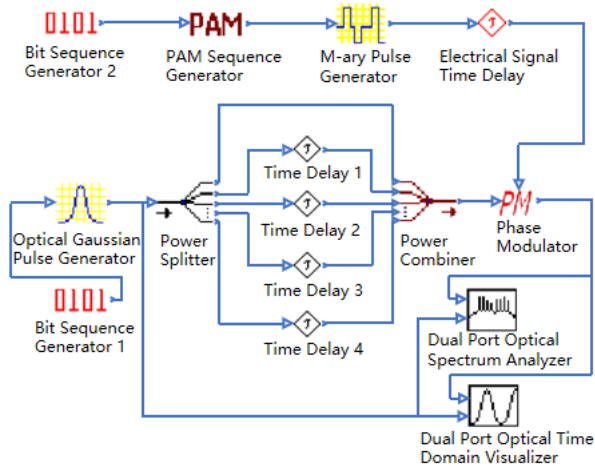


Fig.4 Simulation setup to accomplish the arbitrary FSR control based on an OTDL structure cascaded with a phase modulator, where $N=5$, $s=1$ and $m=2$

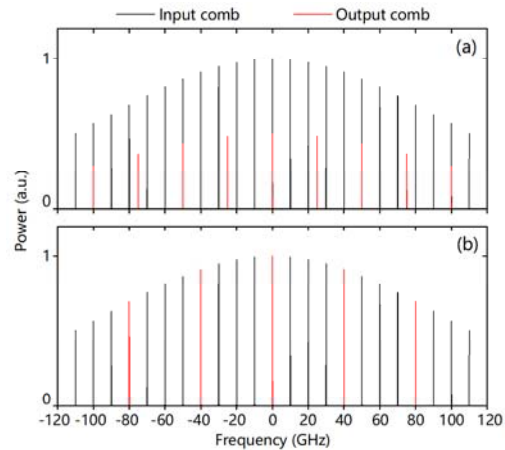


Fig.5 Simulation results for multiplication of FSR: (a) 2.5-times multiplication of FSR; (b) 4-times multiplication of FSR

The simulation results for multiplying the FSR of the input OFC are shown in Fig.5. Fig.5(a) shows the case for the fractional FSR multiplication ($N=5$, $s=1$, $m=2$). In this case, the FSR of input comb is multiplied to 50 GHz through the SAF implemented by a five-tap OTDL structure. And then according to Eq.(2), the periodic phase sequence $\{0, \pi/2, 0, \pi/2, \dots\}$ is applied to the obtained pulse train, which brings about the SSI. Finally, we obtain a comb with FSR equal to 25 GHz, corresponding to the 2.5-times multiplication of the original FSR. Fig.5(b) presents the case for the integer FSR multiplication ($N=4$, $s=0$). It can be seen that the FSR of output comb is increased to 40 GHz from the initial 10 GHz, achieving 4-times multiplication of FSR.

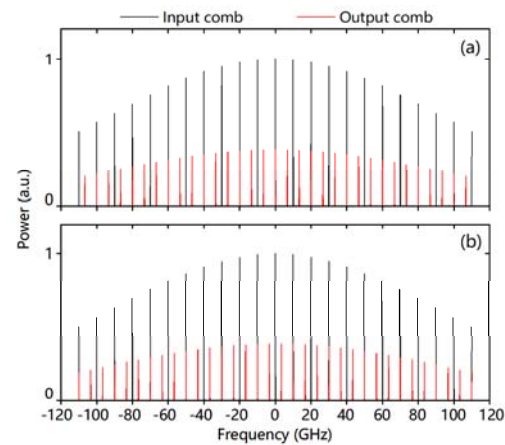


Fig.6 Simulation results for dividing the FSR by a fractional factor (2/3): (a) Normal output comb (red lines); (b) Shifted output comb (red lines)

The simulation results for dividing the input comb

FSR are illustrated in Fig.6. Fig.6(a) and (b) show two different cases, ($N=2, s=3, m=3$) and ($N=2, s=1, m=3$), for the same fractional FSR division factor ($2/3$). The FSRs of both input combs are multiplied to 20 GHz through the two-tap OTDL structure. According to Eq.(2), we know that the periodic phase sequences for the two cases have a difference. The phase sequence in the first case is $\{0, 2\pi/3, 2\pi/3, 0, 2\pi/3, 2\pi/3, \dots\}$, and that in the second case is $\{0, \pi/3, 4\pi/3, \pi, 4\pi/3, \pi/3, 0, \pi/3, 4\pi/3, \pi, 4\pi/3, \pi/3, \dots\}$. Finally, we can see that the FSRs of both output combs are decreased to $20/3$ GHz, but the output comb in Fig.6(b) is shifted by $10/3$ GHz (i.e. half of the FSR) compared with that in Fig.6(a) since the value of ($s \cdot m$) is odd. From the view of OFC control, this also gives us additional ability to change the location of output comb.

Besides, we discuss and simulate the effect of time-delay deviation on output comb spectrum via introducing a certain percentage of deviation (proportional to the corresponding time delay), while keeping other conditions the same as the previous examples. The corresponding output OFC is similar to that shown in Figs.5 and 6, but in the output comb lines, as expected, we find noise, which increases as delay deviation increases. As an example, Fig.7 shows the evolution of the output OFC for $N=5, s=1, m=2$ when Δt (the percentage deviation of each delay line) is varied from 0 to 2.5%, in steps of 0.5%. The simulation results reveal that the output OFC is insensitive to delay deviation if the deviation is less than the certain value (e.g., 2.5% in the given example). We also find that the comb lines that are further from the center frequency vary more significantly under the same deviation. The characteristic can be explained by the fact that the OTDL structure becomes nonuniformly-spaced photonic microwave delay-line filter when delay deviation is non-negligible^[19]. In addition, phase-induced intensity noise (PIIN), which has been studied in optical delay-line signal processor^[20,21], is the dominant noise source in the proposed system. As the SSI effect does not alter the uncorrelated noise background^[10], the PIIN at the output of the system is almost the same as that at the output of spectral amplitude filter. In the frequency domain, the PIIN will result in slight intensity fluctuation of the output comb spectral envelope, which is related to the phase noise of input source.

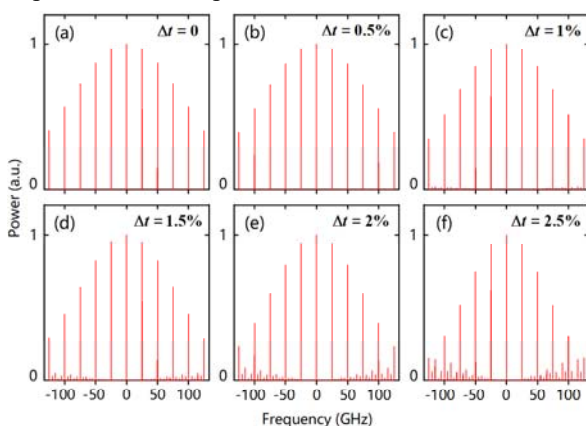


Fig.7 Simulation results for researching the effect of optical delay line inaccuracy on the output OFC, output combs for the percentage deviation of each delay line $\Delta t=0, 0.5\%, 1\%, 1.5\%, 2\%, 2.5\%$, respectively, where $N=5, s=1$ and $m=2$

In conclusion, a simple approach for arbitrary FSR control of OFC has been proposed and demonstrated. The scheme involves the combination of SAF and SSI effect. An OTDL structure is exploited to perform the SAF for the integer multiplication of FSR, and a PM driven by multilevel electrical signal is exploited to perform SSI for the integer division of FSR. In this way, the FSR of output OFC could be set to any anticipated fractional or integer multiple of initial FSR. Several examples, including 4-times multiplication, 2.5-times multiplication and fractional FSR division ($2/3$), have been demonstrated. The simulation results match well with our theoretical analysis. This proposed method expands the variation range of the FSR of input OFC so that one can adjust the FSR more finely and flexibly, which can find numerous potential applications in optical communications, optical signal processing and high-resolution spectroscopy.

References

- [1] P. Ghelfi, F. Laghezza, F. Scotti, G. Serafino, A. Capria, S. Pinna, D. Onori, C. Porzi, M. Scaffardi, A. Malacarne, V. Vercesi, E. Lazzeri, F. Berizzi and A. Bogoni, *Nature* **507**, 341 (2014).
- [2] T. Wilken, G. L. Curto, R. A. Probst, T. Steinmetz, A. Manescau, L. Pasquini, J. I. González Hernández, R. Reboloto, T. W. Hänsch, T. Udem and R. Holzwarth, *Nature* **485**, 611 (2012).
- [3] G. Millot, S. Pitois, M. Yan, T. Hovhannisyan, A. Bendahmane, T. W. Hänsch and N. Picqué, *Nat. Photonics* **10**, 27 (2016).
- [4] T. Udem, R. Holzwarth and T. W. Hänsch, *Nature* **416**, 233 (2002).
- [5] Liu Li, Xu Tie-feng, DAI Zhen-xiang, DAI Shi-xun and Liu Tai-jun, *Optoelectronics Letters* **13**, 104 (2017).
- [6] P. J. Delfyett, S. Gee, M.-T. Choi, H. Izadpanah, W. Lee, S. Ozharar, F. Quinlan and T. Yilmaz, *J. Lightwave Technol.* **24**, 2701 (2006).
- [7] J. Caraquitená, M. Beltrán, R. Llorente, J. Martí and M. A. Muriel, *Opt. Lett.* **36**, 858 (2011).
- [8] J. Azaña and M. A. Muriel, *IEEE J. Sel. Topics Quantum Electron.* **7**, 728 (2001).
- [9] A. Malacarne and J. Azaña, *Opt. Express* **21**, 4139 (2013).
- [10] L. Romero Cortés, R. Maram, H. Guillet de Chatellus and J. Azaña, *Phys. Rev. Appl.* **9**, 064017 (2018).
- [11] H. Guillet de Chatellus, L. Romero Cortés and J. Azaña, *Opt. Express* **26**, 21069 (2018).
- [12] M. A. Soto, M. Alem, M. Amin Shoaie, A. Vedadi, C. S. Brès, L. Thévenaz and T. Schneider, *Nat. Commun.* **4**, 2898 (2013).

- [13] D. Hillerkuss, M. Winter, M. Teschke, A. Marculescu, J. Li, G. Sigurdsson, K. Worms, S. Ben Ezra, N. Narkiss, W. Freude and J. Leuthold, *Opt. Express* **18**, 9324 (2010).
- [14] S. Min, Y. Zhao and S. Fleming, *Opt. Commun.* **277**, 411 (2007).
- [15] Y. Xie, L. Zhuang and A. J. Lowery, *Nanophotonics* **7**, 837 (2018).
- [16] S. Liao, Y. Ding, J. Dong, T. Yang, X. Chen, D. Gao and X. Zhang, *Opt. Express* **23**, 12161 (2015).
- [17] L. Romero Cortés, H. Guillet de Chatellus and J. Azaña, *Opt. Lett.* **41**, 340 (2016).
- [18] C. Rodríguez Fernández-Pousa, *J. Opt. Soc. Am. A* **34**, 732 (2017).
- [19] Y. Dai and J. Yao, *Opt. Express* **16**, 4713 (2008).
- [20] J. Capmany, B. Ortega and D. Pastor, *J. Lightwave Technol.* **24**, 201 (2006).
- [21] E. H. W. Chan and R. A. Minasian, *J. Lightwave Technol.* **27**, 5127 (2009).